

GA-A20238

VERTICAL STABILITY, HIGH ELONGATION, AND THE CONSEQUENCES OF LOSS OF VERTICAL CONTROL ON DIII-D

by

A.G. KELLMAN, J.R. FERRON, T.H. JENSEN,
L.L. LAO, E.A. LAZARUS,* J.B. LISTER,†
J.L. LUXON, D.G. SKINNER, E.J. STRAIT,
E. REIS, T.S. TAYLOR, and A.D. TURNBULL

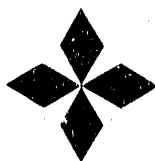
This is a preprint of a paper to be presented at the
Sixteenth Symposium on Fusion Technology, September
3-7, 1990, in London, England and to be printed
in the *Proceedings*.

Work supported by
U.S. Department of Energy
Contract DE-AC03-89ER51114

* Oak Ridge National Laboratory.

† Centre de Recherches en Physique des Plasmas, Association Euratom — Confederation
Suisse, Lausanne, Switzerland.

GENERAL ATOMICS PROJECT 3466
SEPTEMBER 1990



GENERAL ATOMICS

MASTER
DISTRIBUTION OF THIS DOCUMENT IS UNLIMITED

VERTICAL STABILITY, HIGH ELONGATION, AND THE CONSEQUENCES OF LOSS OF VERTICAL CONTROL ON DIII-D

A.G. KELLMAN, J.R. FERRON, T.H. JENSEN, L.L. LAO, E.A. LAZARUS,* J.B. LISTER,† J.L. LUXON, E. REIS, M.J. SCHAFFER, D.G. SKINNER, E.J. STRAIT, T.S. TAYLOR, and A.D. TURNBULL

General Atomics, P.O. Box 85608, San Diego, California 92186-9784, USA ...

*Oak Ridge National Laboratory.

†Centre de Recherches en Physique des Plasmas, Association Euratom - Confederation Suisse, Lausanne, Switzerland.

Recent modifications to the vertical control system for DIII-D has enabled operation of discharges with vertical elongation κ , up to 2.5. When vertical stability is lost, a disruption follows and a large vertical force on the vacuum vessel is observed. The loss of plasma energy begins when the edge safety factor q is 2 but the current decay does not begin until $q \sim 1.3$. Current flow on the open field lines in the plasma scrapeoff layer has been measured and the magnitude and distribution of these currents can explain the observed force on the vessel. Equilibrium calculations and simulation of this vertical displacement episode are presented.

1. INTRODUCTION

One possible approach for improving the tokamak as a candidate for a practical fusion energy device is to vertically elongate the plasma cross-section. There are two primary advantages to high elongation discharges, increased β values ($\beta \sim$ (thermal energy/magnetic energy)) and improved energy confinement time. However, operation at high elongation has negative consequences including an inherent vertical position instability which requires a feedback control system for stabilization. If vertical stability is lost, the result is a termination of the discharge which introduces forces on the vacuum vessel which are different and more severe than those normally experienced during plasma disruptions. This type of termination is called a "vertical displacement episode".

In DIII-D, we routinely operate high elongation single and double null divertor discharges and recent modifications to the vertical control system have made it possible to obtain discharges with elongation up to 2.5. Section 2 of this paper will examine the control problems and vertical stability limits of this high elongation regime. Section 3 describes the phenomenology of a vertical displacement episode and the physical processes and plasma equilibria which correctly account for the observed disruption forces.

2. VERTICAL STABILITY AND PLASMA CONTROL

A model of the plasma vertical stability has been developed¹ which is based on the dynamics of a rigid

body motion of a massless plasma represented by a single current filament. The model includes the effects of active control coils and decomposes the vessel currents in an eigenmode expansion. The most important result of this study is that the active control coil must be positioned so as to minimize its interaction with the stabilizing vessel currents. As a consequence of toroidicity, these currents flow primarily in the outboard regions of the vessel. Thus, the control coils must be positioned on the inboard side of the vessel, near the midplane. Additionally, it was found that the power supply voltage requirement scales exponentially with the plasma decay index ($n = -(R/B_z)(dB_z/dR)$), and the bandwidth requirement is the open loop growth rate of the instability in the plasma-shell-active coil system. It is found that the open loop growth rate is extremely sensitive to the placement of the active coil.

Based on this model, a modified control system was implemented on DIII-D which has permitted operation up to the ideal MHD stability limit. The system utilizes a slow radial field provided by outboard coils and a faster, but weaker field provided by two pairs of inboard coils. A set of detailed measurements of the step response of the control system confirmed the adequacy of this simple control model.² In particular, it was shown in Ref. 2 that the use of the inboard coils was superior and that the plasma-shell-active coil system exhibits a second-order response, in agreement with the model. The highest elongation achieved was 2.5. This limitation to elongation has been explored and we

find that the onset of non-rigid behavior is responsible.³ Although the control system is based on a rigid-body model, it allows operation close to the ideal limit even when these non-rigid effects play a significant role in the evolution of the instability.

In order to improve the flexibility and accuracy of our present shape control while maintaining vertical stability, a high speed digital control system is being designed to replace the analog system now in use. The advantage of the new system is that it allows the continual update of coefficients in the control matrix for more accurate shape control and of the controller gains for more optimal plasma position response. The shape control algorithm is based on a linear regression analysis of 100 magnetic measurements to provide a representation of 18 plasma shape parameters. The required matrix multiplication will be performed by an Intel 80860 microprocessor which has a speed of 80 MFLOPS. The entire control algorithm should be capable of providing updates of control signals in less than 100 μ sec.

3. VERTICAL DISPLACEMENT EPISODES AND MAJOR DISRUPTIONS

For the purpose of this paper, disruptions will be divided into two broad types, major disruptions and vertical displacement episodes (VDEs). In a major disruption, vertical position control is maintained during the thermal quench, though control may be lost after the quench. In a vertical displacement episode, a loss of vertical position precedes the thermal quench.

A major consequence of VDEs is that there is a significant net vertical force on the vacuum vessel and its internal components. On DIII-D, vertical motion of the vacuum vessel is observed with amplitudes of up to 2 mm. This force can arise from the interaction of the poloidal field with toroidal vessel currents or the toroidal field with poloidal vessel currents. Poloidal vessel currents associated with currents on open field lines was suggested by Jensen and Chu⁴ as an important element of VDEs. The physical mechanism responsible for driving these currents will be discussed later.

To determine the magnitude of these currents and associated forces, a model of plasma equilibrium during a VDE was developed. The DIII-D equilibrium code, EFIT, was modified to permit current flow in the plasma scrapeoff layer on open fields which intercept the vessel wall.⁵ The plasma on the open field lines is assumed to be pressureless so that the current is parallel to the field ($j \times B = \nabla p = 0$). For calculation of the

equilibrium using EFIT, 27 adjustable parameters are used of which three specify the current and pressure profile and the remainder specify the toroidal current in 24 vessel segments. The quantity χ^2 measures the difference between the magnetic measurements of the experimental equilibrium and the EFIT equilibrium and the parameters are adjusted to minimize χ^2 . The scrapeoff layer width is specified by a parameter, α , where $\alpha = 1$ corresponds to no scrapeoff layer and $\alpha=0$ to a layer which extends either to the vessel wall or the first separatrix outside the last closed flux surface, whichever is closer. α is varied from 0 to 1 to obtain the best fit. During the VDEs, the minimum in χ^2 is significantly smaller than χ^2 corresponding to $\alpha = 1$ indicating the existence of these currents is essential for a correct description of the equilibrium.

Verification of this model has been obtained through direct experimental measurement of the poloidal currents flowing from the plasma, through the divertor tiles into the vacuum vessel.⁶ The currents are measured by a Rogowski loop around the base of the tile and these measurements have been confirmed with a second independent measurement using a low resistance shunt resistor from an insulated tile to the vessel. An example of the agreement between the current determined from EFIT and the measured currents is shown in Figure 1. Also shown are examples of the equilibria determined by EFIT according to the procedure outlined above. Additional confirmation of the model has been provided by using a detailed engineering model to calculate the vessel displacement. Using the time dependent output of the EFIT code as input for the simulation, a maximum displacement of 0.6 mm was predicted for the discharge shown in Figure 1, which compares well with the measured displacement of 0.5 mm. For typical DIII-D disruptions, 80% of the displacement is due to the interaction of the poloidal current with the toroidal field and the toroidal vessel current plays a relatively small role.

For both major disruptions and VDEs, the start of the plasma current decay occurs after the loss of thermal energy. However, the thermal quench and subsequent current quench during a VDE generally do not occur until the vertical position is far from the centered equilibrium position. The vertical position and other plasma quantities determined using the modified equilibrium code are shown in Figure 2. The SXR signal is included for a time reference. Using the vertical position of the magnetic axis, we find that the once the

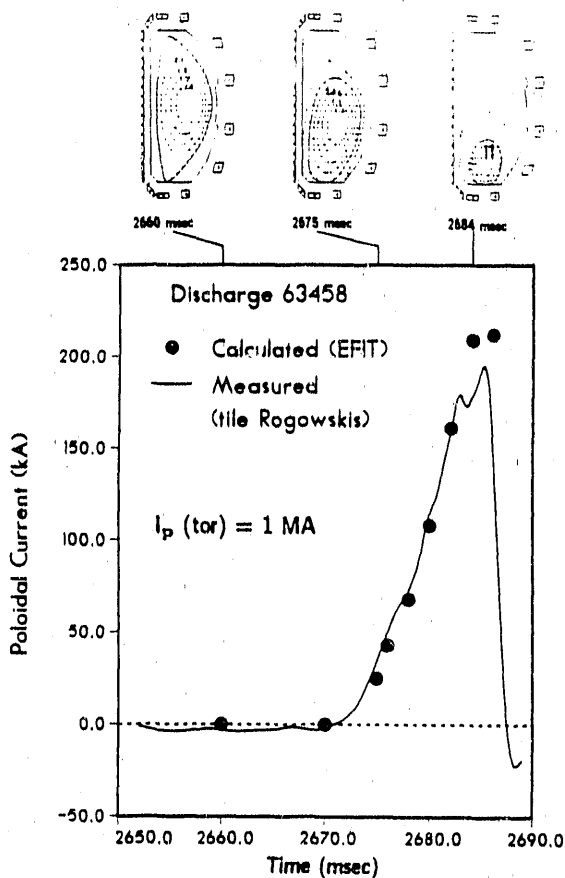


FIGURE 1
Comparison of measured and calculated poloidal scrapeoff layer current. The poloidal currents are contained in the shaded region surrounding the last closed flux surface.

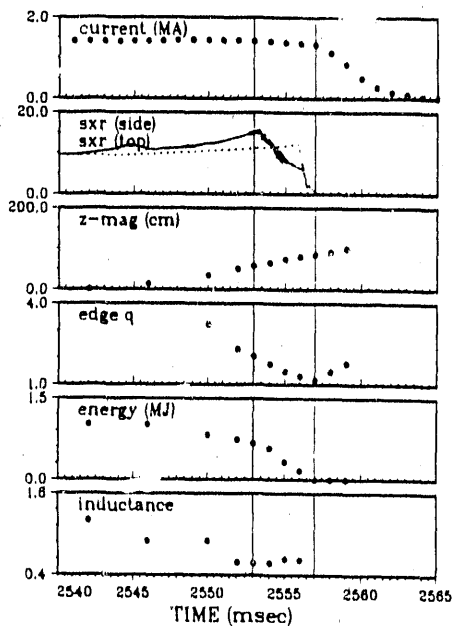


FIGURE 2
Plasma parameters during a vertical displacement episode.

vertical motion starts, the plasma continues to move in one direction without reversal and the current decay does not occur until the plasma is almost 100 cm above the vessel midplane.

More significant than the actual distance from the midplane is that the edge safety factor at the last closed flux surface is significantly below 2.0 at the time the current decay phase begins. During the period when the plasma is drifting vertically upward with constant current, there is a small decrease in the stored energy while the edge safety factor remains above 2.0. In other discharges, the decrease in energy can be as low as 10% during this phase. Once q drops below 2 at 2553 ms, there is a more rapid decrease in the thermal energy. The onset of fluctuations on the SXR signal coincides with the decrease in q below 2 and the decrease in the emission level from the top-viewing chord follows the decrease in the plasma thermal energy during this period. The loss of plasma energy continues until 2556 ms when a rapid crash in the SXR emission occurs as seen on both the side and top viewing chords. This basic scenario is seen on all other discharges we have examined, although, sometimes the rapid crash of the SXR signal is associated with the rapid loss of as much as 30% of the original plasma stored energy. In all cases, this final drop occurs at an edge q of 1.3 to 1.5. It is significant that the energy loss occurs over an interval of 3-4 msec because the plasma continues to move vertically during this period. As a result, it is 20 to 30 cm farther off axis when the thermal quench is complete and the current decay finally begins.

Once the current quench starts, there is an interesting difference between the major disruption and the VDE. In a major disruption, a rapid current increase is typically observed immediately following the thermal quench and preceding the current decay. This current jump is typically 10%-15% of the pre-disruption plasma current and results from the rapid broadening of the current profile at the time of the disruption which lowers the inductance of the discharge. For VDEs, this current jump is not typically observed because the inductance is already low at the time of the thermal quench ($\ell_i \sim 0.5$) and there is very little redistribution of current as thermal energy is lost. However, if a VDE occurs during a rapid rampdown of the plasma current (10 MA/sec), the pre-disruption inductance is much higher and the current jump is observed.

After a major disruption, vertical position control is often lost during the current quench; however,

control has been maintained in some double null divertors after disruptions. It is likely that if discharges are sufficiently up-down symmetric, the vertical displacement can be kept small throughout the entire current decay phase. For the single null divertor which is inherently asymmetric, the discharge always moves in the direction of the X-point following a disruption, while for double null divertors, there is no unique direction for the displacement.

For the purpose of providing guidance in numerical simulation of VDEs, it is important to examine the sensitivity of the plasma parameters determined from EFIT to the width of the scrapeoff layer. Although χ^2 during a VDE improves dramatically with the addition of the scrapeoff layer currents, not all plasma parameters are strongly dependent on the width of the layer (Figure 3)

Two quantities that are relatively insensitive to the scrapeoff layer width are the poloidal and toroidal currents in the layer. In general these vary weakly with α until χ^2 is far from its minimum value. However, there is a stronger dependence of the individual forces on the layer width. The force due to the poloidal vessel currents, F_p , goes to zero as α approaches one because the distance that the current flows in the vessel decreases as the scrapeoff width gets narrower. In contrast, during the period before the current decay starts, the force due to the toroidal vessel current, F_t , increases as α approaches one, so that the sum of the two forces is nearly independent of the layer width. However, once the current decay begins, both the individual forces, F_p and F_t , and their sum depend on α (Figure 3). Since the distribution of the toroidal and poloidal current in the vessel is different, the local stresses on the vessel depend strongly on the layer width, even if the net vertical force is unchanged.

To understand the physical mechanisms that drive both the vessel and scrapeoff layer currents it is useful to divide the VDE into two phases, the drifting phase during which the plasma moves vertically but the plasma current does not decay, and the decay phase which starts after the thermal quench as the total plasma current decays. During the drifting phase, currents are driven primarily by two processes. Toroidal eddy currents are induced in the vessel wall in the sense to oppose the plasma motion. In addition decreasing toroidal flux enclosed by the plasma drives a poloidal current in the scrapeoff layer which is also in the sense to oppose the plasma motion. If the plasma is drifting downward,

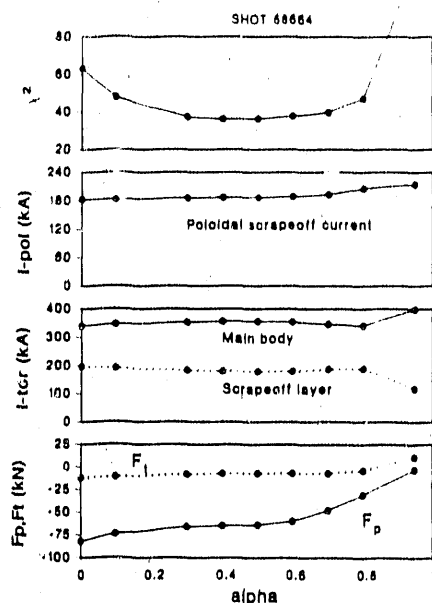


FIGURE 3

Dependence on plasma parameters determined by EFIT as a function of the scrapeoff layer width α . The time chosen, 2807 ms, is during the current decay.

both the poloidal and toroidal vessel currents result in downward forces on the vessel. During the second phase of the VDE, the rapidly decaying plasma current induces a toroidal current in both the vacuum vessel and the scrapeoff layer in the same direction as the original plasma current. Thus, the toroidal vessel current in the region below the plasma actually reverses direction during this decay phase and the force due to the toroidal currents also reverses. The toroidal currents induced in the scrapeoff layer give rise to poloidal currents because the currents are parallel to the total field. These poloidal currents are in the same sense as in the drifting phase, so the force due to the poloidal currents actually increases in magnitude. The actual time behavior of a real discharge is shown in Figure 4. As described above, the reversal of the F_t is observed and this is seen on all DIII-D VDEs. Because F_t reverses sign, its contribution to the total impulse on the vessel is small compared to F_p which is always in the same direction and increases strongly during the decay phase. Numerically, the maximum poloidal current driven is 20% of the pre-disruption plasma current.

It is worth developing a simple scaling model based only F_p during the decay phase since it is responsible for most of the force in DIII-D. If we assume that the characteristic length for the current flow through the vessel is a , the plasma minor radius, then the force

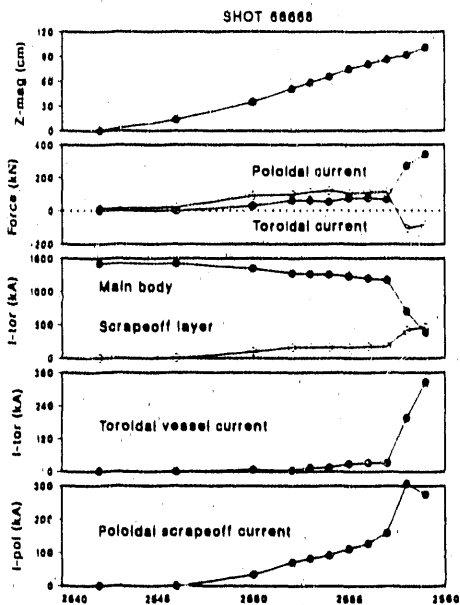


FIGURE 4
Time behavior of position, forces, and currents during a VDE.

on the vessel due to this current is $F_{ves} \sim aI_{pol}B_{tor}$. Since $j \times B = 0$ in the scrapeoff layer, we can relate the poloidal and toroidal currents in this region by $I_{pol} \sim I_{tor}/q$. Since $I_{tor} \sim \gamma I_p$, where I_p is the initial plasma current and γ depends on the resistivity of the scrapeoff plasma, we can rewrite the expression for the force on the vessel as $F_{ves} \sim aI_p B_t/q$. At this point, we invoke the observation that most of the current decay occurs with the a fixed edge q between 1 and 1.5 yielding $F_{ves} \sim aI_p B_t$. In DIII-D, this remarkably simple scaling agrees well with measurements of the vessel displacement.

As a step toward being able to make predictions of disruption forces in future devices, a simulation code has been written to model the dynamics of the VDE.⁷ The model assumes axisymmetric MHD equilibrium and includes parallel currents on the open field lines flowing from the plasma to the vessel. In the plasma region, only the toroidal component of Ohm's law is used. The code results agree well with those obtained by EFIT if the resistivity of the main plasma and scrapeoff layer increase abruptly at the time of the disruption from $\eta \sim 0$

to $\eta \sim 1 - 2 \times 10^{-5} \Omega m$. This corresponds to a Spitzer temperature of approximately 13 to 20 eV at $Z_{eff} = 1$.

In summary, in a VDE the plasma moves vertically in one direction with constant current until the end of the thermal quench phase. Because of the decrease in the plasma size during the vertical motion, the edge q decreases and when it drops below 2, the loss of thermal energy begins. This continues for 3-4 msec at which time the remaining plasma energy is rapidly lost. Since the plasma continues to drift vertically while the energy is being lost, the edge q value at the end of the thermal quench is in the range of 1.3 to 1.5 at which time, the current decay begins. During the drifting phase when q is above 2, there is very little loss of thermal energy, but the internal inductance decreases to 0.5-0.6 indicating a relatively flat current profile at the start of the thermal quench. Currents up to 20% of the initial plasma current have been measured on the open field lines surrounding the main plasma during a VDE and this is in excellent agreement with that obtained by the equilibrium code. The currents have a significant effect on the local distribution of forces on the vessel and the vessel motion on DIII-D can be accounted for by these forces.

ACKNOWLEDGMENT

This work was supported by the U.S. Department of Energy under Contract No. DE-AC03-89ER51114.

REFERENCES

1. E.A. Lazarus, J.B. Lister, G.H. Neilson, Nucl. Fusion 30, 111 (1990).
2. J.B. Lister, E.A. Lazarus, A.G. Kellman, et al., to be published in Nucl. Fusion.
3. E.A. Lazarus, A.D. Turnbull, A.G. Kellman, et al., in Proceedings of the Seventeenth European Conference on Controlled Fusion and Plasma Physics, Amsterdam (EPS, Petit-Lancy, Switzerland, 1990), Vol. I, p. 427.
4. T.H. Jensen and M.S. Chu, Phys. Fluids B 1, 1545 (1989).
5. L.L. Lao, General Atomics Report GA-A20101 to be submitted to Nucl. Fusion.
6. E.J. Strait, submitted to Nucl. Fusion.
7. T.H. Torkil and D.G. Skinner, to be published in Nucl. Fusion.

- END -

DATE FILMED

11 / 06 / 90

